# SAR AND RADIATION CHARACTERISTICS OF A DIPOLE ANTENNA ABOVE DIFFERENT FINITE EBG SUBSTRATES IN THE PRESENCE OF A REALISTIC HEAD MODEL IN THE 3.5 GHz BAND

## R. Ikeuchi, K. H. Chan, and A. Hirata[*]

Department of Computer Science and Engineering, Nagoya Institute of Technology, Showa-ku, Gokiso-cho, Nagoya 466-8555, Japan

**Abstract**—This study investigates the performance of a dipole antenna above electromagnetic band gap (EBG) substrates with different number of patches to realize a low specific absorption rate (SAR) antenna for a 4G wireless communications system (3.5 GHz band). A cubic head model is used for the initial analysis to estimate the radiation characteristics and the SAR of the antenna. Computational results have shown that the antenna above an EBG substrate could provide a maximum reduction of 81% in the SAR and a radiation efficiency improvement of 10% when compared with the antenna above a perfect electric conductor (PEC) ground plane. However, the antenna above an EBG substrate with a lower number of patches results in a higher resonance frequency and cannot provide sufficient SAR reduction In both the cubic and realistic head models, a similar tendency was observed in the SAR reduction capability of the antenna above the EBG substrates when compared with the antenna above the PEC ground plane. For the realistic head model, the SARs of the dipole above EBG substrates with 20 or 24 EBG patches can be reduced by 16% when compared to the case with 12 or 16 EBG patches. The variability of the SAR in the operating frequency band $(|S_{11}| > 10\,\mathrm{dB})$ of the antenna is 5–35% for different EBG substrates.

## 1. INTRODUCTION

Much attention has been paid to the adverse health effects due to electromagnetic (EM) wave exposure from mobile handsets used in proximity to the human head. Hence, safety guidelines for EM

wave exposures have been established by international standardization bodies [1, 2]. The specific absorption rate (SAR) averaged over 10 g of tissue is used as a metric for human safety against localized exposure because it correlates to the temperature elevation in human body [3]. The SAR limit for the general public environment is 2.0 W/kg as prescribed in the international guidelines and standards [1, 2].

A handset with a compact antenna having low SAR and high radiation efficiency characteristics are the essential requirements for mobile phone design in recent years. To satisfy these requirements, several approaches [4, 5] have been proposed and experimented in the last decade. Chan et al. [4, 5] found that the SAR value is affected by various parameters such as the attachment positions of conductive materials and the size and configuration of the antenna ground plane. Some studies inserted a reflector between the radiator and the head [6, 7] for SAR reduction. Other studies applied ferrite sheets [8, 9] shielding materials [10], resistive sheets [11], and artificial magnetic conductors [12] to reduce the EM field around the antenna. Recently, metamaterials, including electromagnetic band-gap (EBG) structures [13], have been proposed for handset antennas with low SAR characteristics [14–16]. According to these studies, the overall dimensions of the antennas with metamaterials were larger than those of the wireless terminals; metamaterial-based antennas were suggested to have dimensions of 45 mm $\times$ 45 mm $\times$ 6 mm for an SAR reduction of 45% at maximum [15]. In fourth-generation (4G) wireless communications systems, much attention is paid to the application of EBG structures to handsets [17]. One of the rationales for this attempt is that the size of the EBG structure is comparable to the wavelength, and thus becomes suitable even for handsets, at the frequency band assigned for 4G systems. Hence, the use of an EBG substrate for antennas in 4G mobile handsets may be one of many possible solutions. In particular, we have investigated the feasibility of using a dipole antenna above the EBG substrate consisting of 24 (4 $\times$ 6) patches in the 3.5 GHz band [18].

In most of the previous studies on EBG structures, a sufficient number of EBG patches were considered [19–21] such that the EBG structures behave as a periodic high-impedance structure. The sizes of these structures may not be sufficiently small for some practical applications such as mobile devices. Further investigation is needed to reduce the size of the antenna above the EBG substrate for wireless terminals. There is, however, no study that discusses the effect of the number of patches on the antenna performance as far as the authors know. In this paper, we present the effect of the number of EBG patches on the radiation characteristics and SAR reduction

capability of the dipole antenna placed above EBG substrate, with the aim of implementing the EBG substrate for wireless terminals. On the basis of the results obtained for the antenna resonance frequency and bandwidth, accurate analysis of the SAR was performed using a high resolution anatomical human head model consisting of 51 tissues. We employed the SAR averaging scheme provided in the Annex E of IEEE C95.3 standard [22]. Herein, we also discuss the peak SAR in an anatomical human head model within the lower, center, and upper operating frequency bands of the antenna, which has not been covered in previous investigations.

## 2. MODEL AND METHOD

### 2.1. Antenna with EBG and Model Geometry

Figure 1 illustrates the geometry of the dipole antenna above the EBG substrate used in our investigation. The dipole length is 43 mm and its radius is 0.2 mm, so that the driven frequency in free space is
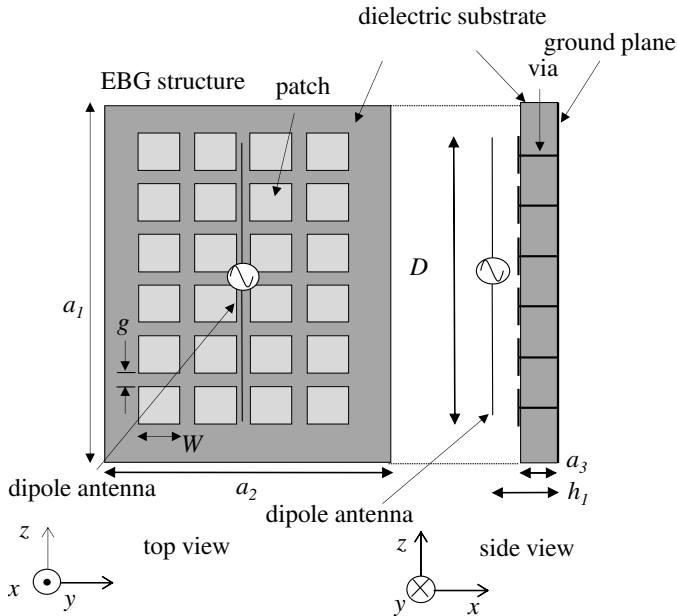


**Figure 1.** Geometry of the dipole antenna on the EBG substrate. $a_1 = 51$ mm, $a_2 = 35$ mm, $a_3 = 3$ mm, $D = 43$ mm, $W = 7$ mm, $g = 1$ mm, $h_1 = 4.5$ mm.

3.5 GHz. A mushroom type EBG [13] was considered because of its simple structure. This structure introduces an inductor $L$, resulting from the current flowing through the via, and a capacitor $C$, due to the gap effect between adjacent patches. For the structure with patch width $W$, gap width $g$, substrate thickness $h$, and dielectric constant $\varepsilon_r$, the values of $L$ and $C$ can be approximated by the formulas given below [10]:

$$L = \mu_0 h \tag{1}$$

$$C = \frac{W \varepsilon_0 (1 + \varepsilon_r)}{\pi} \cosh^{-1} \left( \frac{2W + g}{g} \right) \tag{2}$$

$$\varpi = \frac{1}{\sqrt{LC}} \tag{3}$$

where $\mu_0$ and $\varepsilon_0$ are the permeability and permittivity of free space. From the equivalent inductance and capacitance obtained from Eqs. (1) and (2), the approximate center frequency of the band gap $\varpi$ can be obtained from Eq. (3).

The dimensions of the ground plane are set at $35\,\text{mm} \times 51\,\text{mm}$, so that the dimension is small enough to fit a handset. The relative permittivity of the substrate $\varepsilon_r$ is chosen to be 10.2, corresponding to Rogers RT/Duroid 6010 laminates. As mentioned in Section 1, the number of EBG patches is reduced in order to investigate its effect on the antenna performance. Fig. 2 shows a diagram of five EBG substrates with 24, 20, 16, 12 and 4 patches used in our analysis.

Figure 3 illustrates the geometry of the dipole antenna in close proximity to a homogeneous cubic model. A cubic model comprised of the muscle was considered here to investigate the radiation characteristics of the proposed structure [23]. The dimensions of the head model are $70\,\text{mm}\,(x) \times 200\,\text{mm}\,(y) \times 200\,\text{mm}\,(z)$. The model reduction in the $x$ direction is due to the small penetration depth



EBG-1        EBG-2        EBG-3        EBG-4        EBG-5

24 Patches    20 Patches    16 Patches    12 Patches    4 Patches
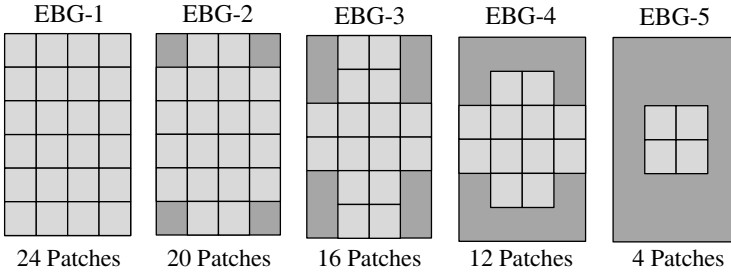
**Figure 2.** Diagram of the dielectric substrates with different number of patches.
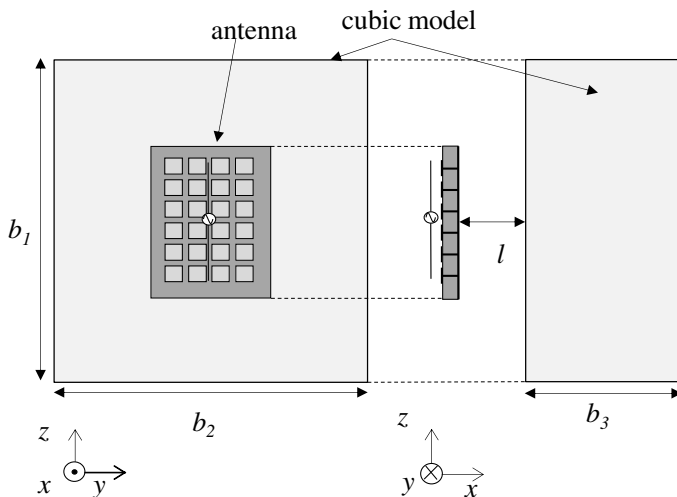
**Figure 3.** Geometry of the antenna and cubic head model. $l = 10\,\text{mm}$, $b_1 = b_2 = 200\,\text{mm}$, $b_3 = 70\,\text{mm}$.

of electromagnetic waves at 3.5 GHz [24]. The electrical constants for muscle were taken from a previous report [25].

After obtaining the initial results from the cubic model, we verified the performance of the proposed antenna with an anatomical human head model comprised of 51 tissues [26]. Fig. 4 shows the geometry of the antenna in close proximity to the head model truncated from the anatomical human head model. Only the head and neck were used in the present study because the antenna has a small size and it was located at the position near the human head where an earpiece would be. The width, depth, and height of the anatomic head model are 198 mm, 212 mm, and 260 mm, respectively. The electrical constants for the tissues were taken from a previous report [25]. In order to keep the computational accuracy and reliability of the model as high as possible, a high resolution of $0.5\,\text{mm} \times 0.5\,\text{mm} \times 0.5\,\text{mm}$ for the anatomical human head model was used in our investigation.

## 2.2. Computational Method

The finite-difference time-domain (FDTD) method was employed to calculate the EM wave and lossy dielectric interaction. One of the primary reasons for using the FDTD method is its stability for a finite dielectric substrate as compared to that of the method of moments
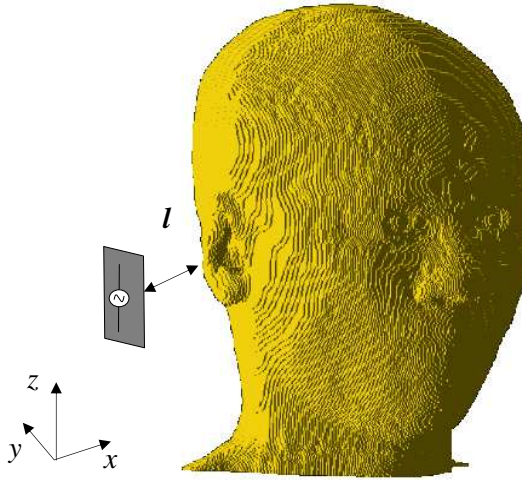
**Figure 4.** Geometry of the antenna in close proximity to an anatomical human head mode ($l = 10$ mm).

(MoM). The resolution of the cell was $0.5$ mm $(x) \times 0.5$ mm $(y) \times 0.5$ mm $(z)$. This resolution is chosen so that the gap width of the structure has at least two cells in the model. To terminate the computational region, a 12-layered perfectly matched layer absorbing boundary was used. The SAR is calculated using the following formula:

$$SAR = \frac{\sigma E^2}{\rho} \qquad (4)$$

where $\sigma$ is the electrical conductivity, $\rho$ is the mass density, and $E$ is the internal electric field strength. An algorithm suggested in the IEEE standard [22] was used to compute the averaged SAR over 10 g of tissue, which is a metric for human safety [1, 2]. Note that the pinna was treated as an extremity and thus the pinna was excluded from the averaging region. The radiated output power of the dipole antenna was set to $1.0$ W. For a lower radiated output power requirement in future 4G systems, the SAR value can be obtained using the proportional relationship between the radiated power and the SAR value.

To validate our computational results for the SAR and antenna performance analysis of the homogenous cubic model with the FDTD method, a hybrid MoM/FEM method available in the commercial software package FEKO was used [27]. Following this, the FDTD method was used for investigating the SAR value for the homogeneous and realistic anatomic head model.
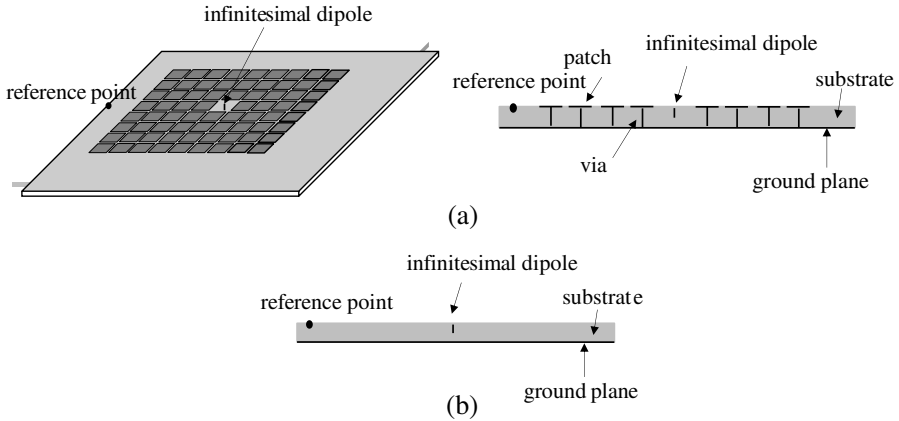
**Figure 5.** The FDTD simulation model consisting of an infinitesimal dipole source surrounded by (a) mushroom-like EBG substrate, and (b) PEC with substrate.

# 3. COMPUTATIONAL RESULTS AND DISCUSSION

## 3.1. Validation of the Surface Wave Suppression Characteristics of an EBG

To identify the band gap region and demonstrate its properties comprehensively, we constructed a FDTD simulation model consisting of an infinitesimal dipole source surrounded by mushroom-like EBG patches as shown in Fig. 5(a). A similar model without any mushroom-like EBG patches and pins was also constructed as illustrated in Fig. 5(b) for comparison. In both cases, the dimensions and material properties of the ground plane and substrate were identical and consistent with those in Fig. 1.

The basic idea for constructing this model is to calculate and compare the electric field at the reference point located outside the region of EBG patches. Because the EBG structure can suppress surface waves within a certain band gap, the electric field at the reference point in the EBG must have a lower value than that in a perfect electric conductor (PEC).

To determine the band-gap region, the criteria that the average electric field magnitude at the reference point in the EBG case should be less than half of that in the PEC case [12] was used:

$$20 \log_{10} \frac{|E_{EBG}|}{|E_{PEC}|} \leq -6 \, \text{dB} \qquad (5)$$

where $E_{EBG}$ and $E_{PEC}$ are the average electric fields at the reference
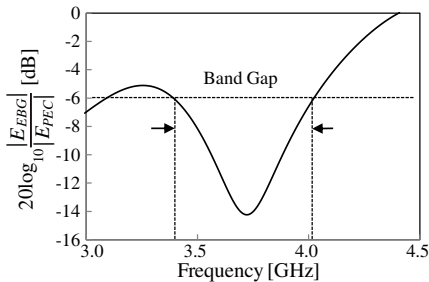
**Figure 6.** Determination of the band gap frequency using the reference point model.
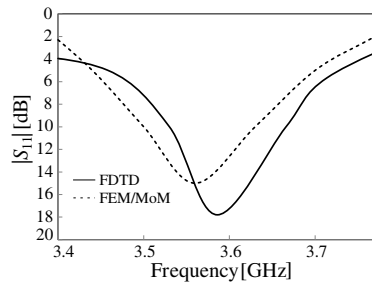


**Figure 7.** $|S_{11}|$ of a dipole antenna above different EBG substrates.

**Table 1.** Bandwidth and center frequency for the dipole antenna placed above the EBG substrate.

|                        | FDTD | FEM/MoM | difference [%] |
|------------------------|------|---------|----------------|
| BW [%]                 | 3.78 | 3.61    | 4.7            |
| Center frequency [GHz] | 3.60 | 3.56    | 1.1            |

point for the EBG and PEC case, respectively. Using Eq. (5), a band gap in the range 3.4–4.1 GHz can be identified as shown in Fig. 6.

## 3.2. Comparison on FDTD Method and FEM/MoM Method

To verify the computational results obtained from the in-house FDTD code, we computed the return loss ($|S_{11}|$) under the same conditions in FEKO [27]. Fig. 7 shows the return loss for the antenna computed by both FDTD and FEM/MoM methods. The bandwidth and center frequency of the antenna in the presence of a head are listed in Table 1. The magnitude of $S_{11}$ is 18 dB at 3.6 GHz computed by the FDTD method, while it is 14 dB at 3.56 GHz computed using FEKO. The difference in the center frequencies obtained by the two methods is only 1.1%. The computed bandwidth in the two methods was almost identical, with a deviation of 4.7%. This deviation is consistent and much smaller than the differences of 30% observed in the inter-comparisons using FDTD, MoM, and FEM methods of 30% [28]. This tendency was confirmed in the antenna above other EBG substrates with different number of patches, although not shown here to avoid repetition.

### 3.3. Radiation Characteristics

In this part, we focus on the radiation characteristics including the return loss, radiation efficiency, and radiation pattern of the dipole antenna above an EBG substrates with different number of EBG patches.

Figure 8 shows the return loss $|S_{11}|$ for the antenna above different EBG substrates. For comparison, the dipole antennas over a PEC are also considered. The $|S_{11}|$ of the dipole antenna in free space is 20 dB at 3.2 GHz, while the $|S_{11}|$ values of the dipole antenna above different finite EBG substrates are comparable, but the center frequencies are shifted from 3.6 GHz to 4.2 GHz. In general, the center frequency of the antenna is shifted to a higher frequency when the number of EBG patches is decreased. This is because the reflection phases from the EBG substrates are varied [19]. In addition, the EBG patches may not be able to act as a periodic structure for wave suppression when the number of EBG patches is insufficient (EBG-5).

Table 2 summarizes the center frequency and the bandwidth of the dipole antenna above different EBG substrates. The results for the antenna above a PEC are also included in the table for comparison. For the dipole antenna in free space, the operating frequency range is from 3.0 to 3.4 GHz with an $|S_{11}|$ of greater than 10 dB. The bandwidths of the dipole antennas above the EBG-1, EBG-2, EBG-3, and EBG-4 substrates range from 3.8% to 4.5%, as shown in Table 2. This is a well-known narrow bandwidth characteristic when implementing periodic structures for antennas [9]. For the EBG-5 structure consisting of four patches, the size of the antenna can be reduced significantly. However, as shown in Fig. 8, the simulated results indicate that the antenna

**Table 2.** Radiation characteristics and peak 10-g averaged SAR of a dipole antenna above different EBG substrates.

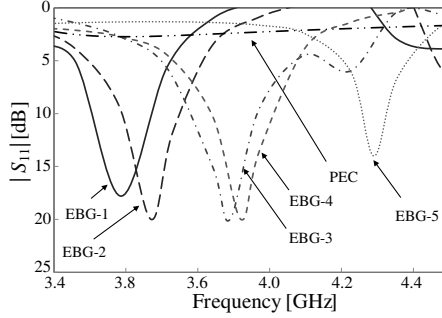| Substrate | CF [GHz] | BW [%] | Radiation Efficiency [%] | Peak 10-g avg SAR [W/kg] | | |
|---|---|---|---|---|---|---|
| | | | | Cubic model | Homogeneous human model | Anatomical human model |
| EBG-1 | 3.59 | 3.78 | 91 | 1.08 | 0.87 | 1.28 |
| EBG-2 | 3.67 | 4.15 | 91 | 1.15 | 0.99 | 1.44 |
| EBG-3 | 3.89 | 4.46 | 92 | 0.99 | 0.97 | 2.09 |
| EBG-4 | 3.92 | 4.08 | 86 | 1.36 | 1.1 | 2.17 |
| PEC | 3.5 | 0 | 82 | 5.15 | 2.99 | 3.04 |

**Figure 8.** $|S_{11}|$ of a dipole antenna above different EBG substrates.

resonance frequency is shifted to 4.3 GHz with a narrow bandwidth of only 1.6%. This reduced bandwidth was not improved if the dimension of patch was adjusted such that the antenna resonance frequency is well within the band gap. Thus, the poor antenna performance for the EBG-5 structure is mainly due to the insufficient number of patches. Hence, the SAR for the EBG-5 structure is not investigated in the following discussion.

The radiation efficiency of the antennas was investigated in order to evaluate the antenna performance. As shown in Table 2, the efficiency of the antenna with the PEC ground plane is 82%. The radiation efficiency can be improved to over 9% when the EBG-1, -2, and -3 substrates are used.

Figure 9 illustrates the radiation patterns for the antenna above the EBG-1 and EBG-4 substrates computed using FEKO. The results indicate that the maximum gain of the antenna above EBG-1 is 6.6 dB, which is located along the positive $x$-axis above the EBG substrate. Similar radiation pattern characteristics have also been obtained for the EBG-2 to EBG-4 substrates with antenna gains of more than 6 dB. According to the results of the antenna patterns, the isolations have more than 26.5 dB in the direction above the ground plane for all the substrates considered here.

## 3.4. SAR in Cubic Model

The peak SAR averaged over 10 g was computed for different EBG substrates in close proximity to the cubic model as shown in Fig. 3. The computed results of the peak SAR averaged over 10 g are summarized in Table 2. For proper comparison, the antenna above the PEC was assumed to be connected with a matched load. The peak SARs averaged over 10 g for the antennas with all of the EBG substrates
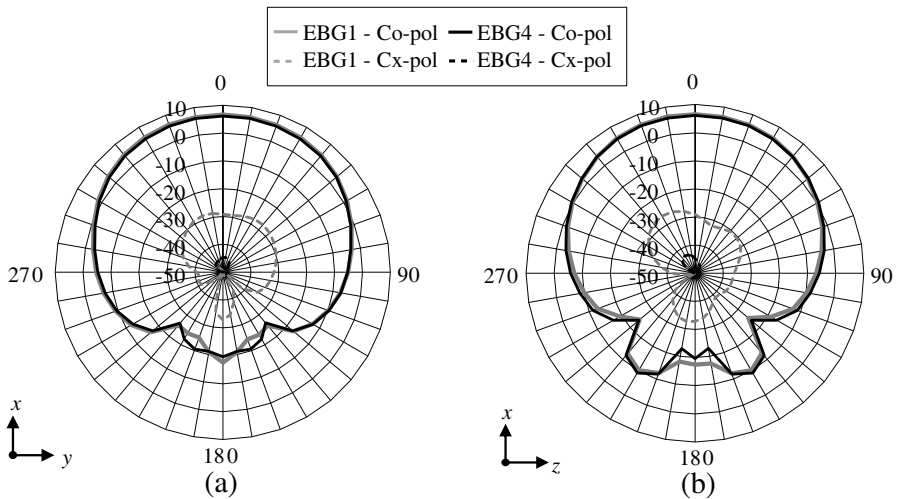
**Figure 9.** Radiation patterns for the EBG-1 and EBG-4 substrates in the (a) $xy$-plane and (b) $xz$-plane.

were lower than the SAR above the PEC. The SAR of the antenna above the EBG-1 substrate was reduced by 81% when compared to the antenna above the PEC ground plane. The main reason for this reduction is caused by the suppression of surface waves by the EBG structure, resulting in the suppression of diffracted waves from ground plane.

Figure 10 shows the voxel SAR distribution in the head model due to the antenna with the EBG-1, -2, -3 and -4 substrates and PEC ground plane. As seen from Fig. 10(e), the SAR distribution is concentrated behind the ground plane for the antenna above the PEC. On the contrary, the SAR value becomes higher at both sides of the substrate due to diffracted waves. This tendency was also shown in the antenna above other EBG substrates.

## 3.5. SAR for the Anatomical Human Head Model and Variability of SAR in the Operating Frequency Band

To investigate the variability of the SAR in human head models, the peak SAR averaged over 10 g was computed for the anatomical human head model. The resulting SAR caused by the antenna above the PEC ground plane operating at the center frequency was also calculated for comparison, and the computed results are summarized in Table 3. The results show that the averaged SARs for the dipole above the
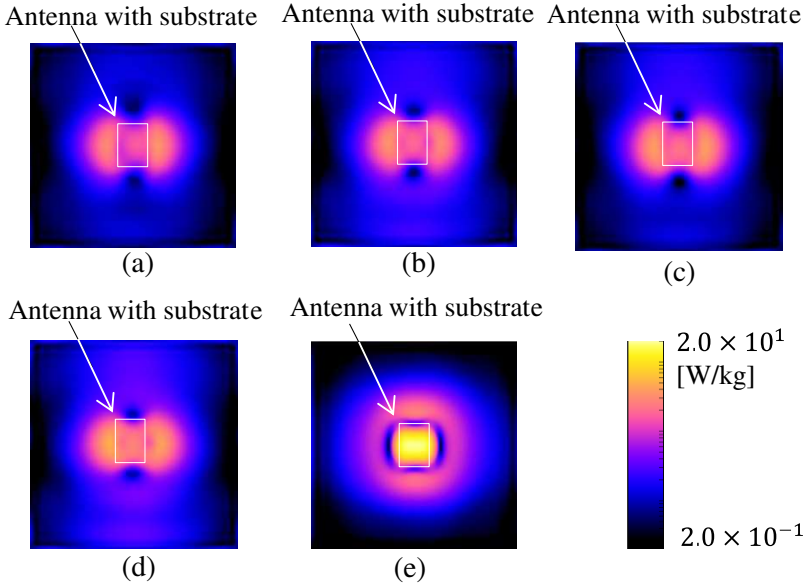
**Figure 10.** SAR distributions for the cubic model with the antenna above the (a) EBG-1, (b) EBG-2, (c) EBG-3, (d) EBG-4, and (e) PEC structures.

EBG-1 and EBG-2 substrates are 16% lower than that of the EBG-3 or EBG-4 substrates. One of the primary reasons for this tendency is due to the geometry of the EBGs. The number of cells located on the edge and parallel to the dipole was reduced for the EBG-3 and EBG-4 substrates. Therefore, the number of patches used for the EBG-3 and EBG-4 substrates may not be enough to suppress surface wave propagation. However, the SAR for the dipole above the PEC ground plane is still higher than the SAR above the EBG substrate at all frequencies as indicated in Table 3. This is because surface waves cannot be suppressed for the PEC case. Therefore, the reductions of the SARs for the antenna above the EBG-3 and EBG-4 substrates are sufficient when compared with reduction in the SAR above the PEC ground plane.

As shown in Fig. 11, the SAR varies by 5–35% even in the operating frequency band. The SAR of the antenna above the EBG substrates at the lower, center, and upper operating frequency bands of the antenna was reduced.

**Table 3.** Calculated peak SAR averaged over 10 g in anatomical and homogenous human models for different EBG substrates.

| Substrate | | Anatomical human model | | | Homogeneous human model | | | Differences on SAR between two models [%] |
|---|---|---|---|---|---|---|---|---|
| | | (Lower Freq.) | (Center Freq.) | (Upper Freq.) | (Lower Freq.) | (Center Freq.) | (Upper Freq.) | |
| EBG-1 | Frequency [GHz] | 3.45 | 3.59 | 3.73 | 3.45 | 3.59 | 3.73 | 29.3 |
| | Peak 10-g avg SAR [W/kg] | 1.18 | 1.28 | 1.64 | 0.82 | 0.87 | 1.16 | |
| EBG-2 | Frequency [GHz] | 3.52 | 3.67 | 3.82 | 3.52 | 3.67 | 3.82 | 25 |
| | Peak 10-g avg SAR [W/kg] | 1.29 | 1.44 | 1.84 | 0.88 | 0.99 | 1.38 | |
| EBG-3 | Frequency [GHz] | 3.72 | 3.89 | 4.06 | 3.72 | 3.89 | 4.06 | 40.5 |
| | Peak 10-g avg SAR [W/kg] | 2.20 | 2.09 | 2.10 | 0.87 | 0.97 | 1.31 | |
| EBG-4 | Frequency [GHz] | 3.76 | 3.92 | 4.08 | 3.76 | 3.92 | 4.08 | 48.2 |
| | Peak 10-g avg SAR [W/kg] | 2.20 | 2.17 | 2.01 | 1.06 | 1.1 | 1.41 | |
| PEC | Frequency [GHz] | 3.5 | | | 3.5 | | | 1.6 |
| | Peak 10-g avg SAR [W/kg] | 3.04 | | | 2.99 | | | |
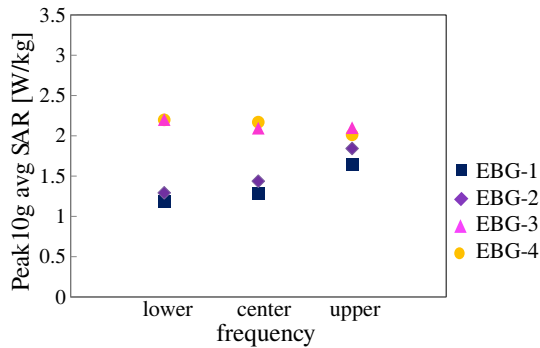


**Figure 11.** Peak 10-g averaged SAR for the dipole antenna above different EBG substrates at relative frequencies satisfying the return loss larger than 10 dB.

## 3.6. Discussion of Differences in SARs for Various Head Models

From the results in Table 2, we found that the estimated SAR values in various head models were different. Specifically, the differences in the SAR values between the cubic and homogenous human head were less than 24% for the EBG-1 to EBG-4 substrates. Our results are consistent with our previous studies [29] which found that the SAR differences in different shapes of human head models are less than 30% at 900 and 1800 MHz. As shown in Table 2, by comparing the SAR values in the cubic and anatomical human models, the differences could be up to 52%.

In order to further confirm the dominant factor affecting the peak averaged SAR, the SAR value for the homogenous human model was considered and listed in Table 3 for comparison. The results illustrated that the differences in two models could be up to 48.2%. The SAR distributions due to the antenna above EBG-1 and EBG-4 substrates for the homogeneous and anatomical human models are also shown in Fig. 12. The SAR distributions in the horizontal plane include the antenna feeding point. The results show that the SAR
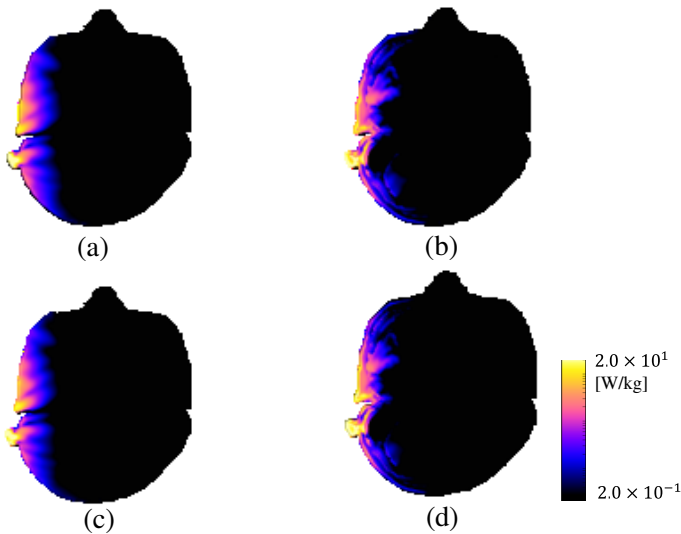


**Figure 12.** SAR distributions due to the antenna above the EBG-1 and EBG-4 substrates for the homogeneous and anatomical human models. (a) EBG-1, homogeneous, (b) EBG-1, anatomical, (c) EBG-4, homogeneous, (d) EBG-4, anatomical.

distribution is different due to the heterogeneity of the model. The SAR in the anatomical human model had a larger value than that in the homogeneous human model. The anatomical composition model could play an important role on the peak averaged SAR at 3.5 GHz. For a SAR averaged over 10 g in a cube with a side length of about 22 mm the penetration depth of electromagnetic waves in human body at 3.5 GHz is around 15 to 20 mm. Therefore, the power absorbed in the model could be affected by the anatomical composition. The reasons for the difference in the SAR value between the cubic and anatomical head models are attributed to both shape and material differences. However, all models indicated that the SAR could be reduced by employing an EBG structure when the number of patches was increased.

## 4. SUMMARY AND CONCLUDING REMARKS

In this paper, the SAR and the radiation characteristics of a 3.5 GHz dipole antenna above a number of different EBG substrates has been examined. The surface wave suppression characteristics and the corresponding band gap region of the EBG structure used in our studies have also been verified. The homogeneous cube along with high resolution homogeneous human and anatomical human models were included in the investigation. Results showed that the SAR for the antenna above the EBG substrates was lower than the SAR for the antenna above PEC ground plane. For the cubic model used in our initial SAR and radiation characteristics analysis, results indicated that the SAR for the antenna above an EBG substrate could be reduced by 81% and the radiation efficiency could be increased by 10%, when compared with the case of an antenna above PEC ground plane. It was also found that the center frequency of the dipole antenna shifted to a higher frequency band and could not provide a good SAR reduction when the number of EBG patches was insufficient. Our results illustrated that the resonance frequency of the EBG structure with four patches shifted to a higher frequency of 4.3 GHz and had a narrow bandwidth of only 1.6%; this structure may not be appropriate for practical purposes. For the anatomical human model we employed the IEEE averaging scheme for the SAR. The induced SAR for the EBG substrates consisting of 20 or 24 patches were 16% lower than the SAR for the EBG substrates with 12 or 16 patches. It was found that the maximum variation in the SAR values within the operating frequency bands for the antenna above different EBG structures could be as high as 35%, which was not investigated in the previous study on the SAR reduction.

Due to the limitations in the SAR analysis requiring a gap length of least 0.5 mm, the thickness of 3 mm was used in this study. Even though this dimension is much smaller than those in previous studies, the antenna dimension can be adjusted on the basis of Eqs. (1), (2), and (3) for an antenna made of a thinner substrate. For example, when the thickness of the PCB is reduced by half, the antenna can attain similar performance by decreasing the gap length to 0.1 mm and increasing the width to 7.9 mm. A similar number of patches for the substrate may be useful in order to increase the width of the patch or to realize an EBG substrate for SAR reduction. Our future work involves designing a more realistic antenna structure for wireless terminals.

# REFERENCES

1. ICNIRP, "Guidelines for limiting exposure to time-varying electric, magnetic and electromagnetic fields (up to 300 GHz)," *Health Phys.*, Vol. 74, 494–522, 1998.

2. IEEE, "C95.1 IEEE standard for safety levels with respect to human exposure to radio frequency electromagnetic fields, 3 kHz to 300 GHz," IEEE, New York, 2005.

3. Hirata, A., K. Shirai, and O. Fujiwara, "On averaging mass of SAR correlating with temperature elevation due to a dipole antenna," *Progress In Electromagnetics Research*, Vol. 84, 221–237, 2008.

4. Chan, K. H., K. M. Chow, L. C Fung, and S. W. Leung, "Effects of using conductive materials for SAR reduction in mobile phone," *Microwave & Opt. Tech. Lett.*, Vol. 44, No. 2, 140–144, 2005

5. Chan, K. H., K. M. Chow, L. C Fung, and S. W. Leung, "SAR of internal antenna in mobile-phone applications," *Microwave & Opt. Tech. Lett.*, Vol. 45, No. 4, 286–290, 2005.

6. Tay, R. Y. S., Q. Balzano, and N. Kuster, "Dipole configurations with strongly improved radiation efficiency for hand-held transceivers," *IEEE Trans. on Antennas & Propagat.*, Vol. 46, 798–806, 1998.

7. Hirata, A., T. Adachi, and T. Shiozawa, "Folded-loop antenna with a reflector for mobile handset at 2.0 GHz," *Microwave & Opt. Tech. Lett.*, Vol. 40, No. 4, 272–275, 2004.

8. Wang, J. and O. Fujiwara, "Reduction of electromagnetic absorption in the human head for portable telephones by a ferrite sheet," *IEICE Trans. on Commun.*, Vol. E80-B, No. 12, 1997.

9. Islam, M. T., M. R. I. Faruque, and N. Misran, "Design analysis

of ferrite sheet attachment for SAR reduction in human head,” *Progress In Electromagnetics Research*, Vol. 98, 191–205, 2009.

10. Fung, L. C., S. W. Leung, and K. H. Chan, “Experimental study of SAR reduction on commercial products and shielding materials in mobile phone applications,” *Microwave & Opt. Tech. Lett.*, Vol. 36, 419–422, 2003.

11. Chou H.-H., H.-T. Hsu, H.-T. Chou, K.-H. Liu, and F.-Y. Kuo, “Reduction of peak SAR in human head for handset applications with resistive sheets (r-cards),” *Progress In Electromagnetics Research*, Vol. 94, 281–296, 2009.

12. Lee S. and N. Kim, “SAR reduction technique by the high impedance surface using the artificial magnetic conductor,” *34th Annual Conference of the Bioelectromagnetics Society*, 49–50, 2012.

13. Yang, F. and Y. Rahmat-Samii, “Microstrip antennas integrated with electromagnetic band-gap (EBG) structures: A low mutual coupling design for array applications,” *IEEE Trans. on Antennas & Propagat.*, Vol. 51, No. 10, 2936–2946, 2003.

14. Manapati, M. B. and R. S. Kshetrimayum, “SAR reduction in human head from mobile phone radiation using single negative metamaterials,” *Journal of Electromagnetic Waves and Applications*, Vol. 23, No. 10, 1385–1395, 2009.

15. Hwang, J.-N. and F.-C. Chen, “Reduction of the peak SAR in the human head with metamaterials,” *IEEE Trans. on Antennas & Propagat.*, Vol. 54, No. 12, 3763–3770, 2006.

16. Kwak, S. I., D. U. Sim, J. H. Kwon, and H. D. Choi, “Experimental tests of SAR reduction on mobile phone using EBG structures,” *Electron. Lett.*, Vol. 44, No. 9, 568–569, 2008.

17. Mahmoud, K. R., M. El-Adawy, S. M. M. Ibrahem, R. Bansal, and S. H. Zainud-Deen, “Investigating the interaction between a human head and a smart handset for 4 g mobile communication systems,” *Progress In Electromagnetics Research C*, Vol. 2, 169–188, 2008.

18. Ikeuchi, R. and A. Hirata, “Dipole antenna above EBG substrate for local SAR reduction,” *IEEE Antennas and Wireless Propagation Letters*, Vol. 10, 904–906, 2011.

19. Yang, F. and Y. Rahmat-Samii, “Reflection phase characterization of the EBG ground plane for low profile wire antenna application,” *IEEE Trans. on Antennas & Propagat.*, Vol. 51, No. 10, 2691–2702, 2003.

20. Barlevy, A. S. and Y. Rahmat-Samii, “Characterization of

electromagnetic band-gaps composed of multiple periodic tripods with interconnecting vias: Concept, analysis, and design," *IEEE Trans. on Antennas & Propagat.*, Vol. 49, 242–353, 2001.

21. Azad, M. Z. and M. Ali, "Novel wideband directional dipole antenna on a mushroom like EBG structure," *IEEE Trans. on Antennas & Propagat.*, Vol. 56, No. 5, 1242–1250, 2008.

22. IEEE, "C95.3-2002 IEEE recommended practice for measurements and computations of radio frequency electromagnetic fields with respect to human exposure to such fields, 100 kHz–300 GHz," *IEEE*, New York, 2002.

23. Kiminami, K., A. Hirata, Y. Horii, and T. Shiozawa, "A study on human body modeling for the mobile terminal antenna design at 400 MHz band," *Journal of Electromagnetic Waves and Applications*, Vol. 19, No. 5, 671–687, 2005.

24. Hirata, A., S. Mitsuzono, and T. Shiozawa, "Feasibility study of adaptive nulling on handset for 4G mobile communications," *IEEE Antennas and Wireless Propagation Letters*, Vol. 3, 120–122, 2004.

25. Gabriel, S., R. W. Lau, and C. Gabriel, "The dielectric properties of biological tissues: III. Parametric models for the dielectric spectrum of tissues," *Phys. Med. Biol.*, Vol. 41, 2271–293, 1996.

26. Nagaoka, T., S. Watanabe, K. Sakurai, E. Kunieda, S. Watanabe, M. Taki, and Y. Yamanaka, "Development of realistic high-resolution whole-body voxel models of Japanese adult males and females of average height and weight, and application of models to radio-frequency electromagnetic-field dosimetry," *Phys. Med. Biol.*, Vol. 49, 1–15, 2004.

27. *FEKO User's Manual*, Suite 4.2, EM Software & Systems (USA), Inc., Hampton, VA, Jun. 2004. [Online]. Available: http://www.feko.info.

28. Beard, B. B., W. Kainz, T. Onishi, T. Iyama, S. Watanabe, O. Fujiwara, J. Wang, G. Bit-Babik, A. Faraone, J. Wiart, A. Christ, N. Kuster, A.-K. Lee, H. Koeze, M. Siegbahn, J. Keshvari, H. Abrishamkar, W. Simon, D. Manteuffel, and N. Nikoloski, "Comparisons of computed mobile phone induced SAR in the SAM phantom to that in anatomically correct models of the human head," *IEEE Trans. on Electromagnet. Compat.*, Vol. 48, No. 2, 397–407, 2006.

29. Chan, K. H., "A study of electromagnetic radiation and specific absorption rate of mobile phones with fractional human head models," Ph.D. Thesis, City University of Hong Kong, 2008.